# Fundamental limits on the losses of phase and amplitude optical actuators

**Simone Zanotto*, Francesco Morichetti, and Andrea Melloni**

## 1. Introduction

In general, the performance of a device is intimately connected through fundamental physical laws to the properties of the materials or the sub-elements employed in the realization of the device, and these connections may have far-reaching implications for whole branches of engineering. For instance, the energy conversion efficiency of a solar cell is limited by several fundamental limits: for photoexcited carrier exploitation, the Shockley–Queisser limit applies [1]; photon trapping inside the absorber is instead governed, in the ray-optics regime, by the Yablonovitch limit [2] or by more general formulas recently proposed by Fan *et al.* [3] for wavelength-size patterned cells.

Focusing back on the optical science, and more specifically on the integrated optical device framework, recent developments are moving towards reconfigurable systems constituted of several elements, in order to implement complex operations on classical or quantum signals [4, 5]. As basic building blocks operating on the amplitude or on the phase of the wave, besides traditional switching elements – like those relying on thermic, electric, or plasma dispersion effects – devices involving novel materials have been under investigation in the recent years. Among them can be cited vanadium dioxide ($VO_2$) [6–11], $Ge_2Sb_2Te_5$ (GST) [12–17], indium tin oxide (ITO) [18, 19], polymeric materials [20], and resistive switches [21]. With these materials, and in connection to other concepts like plasmonic waveguides, it is expected that certain device metrics like miniaturization, speed, energy consumption, and state retention will be improved [22]. However, advantages usually come at a price, and in the present case this can be globally summarized as large losses.

For instance, plasmonic waveguides systematically suffer from large losses, especially in the visible and near-infrared spectral ranges, which are of interest for communications [23]. This does not occur by chance, since the field confinement and the propagation losses are connected by a fundamental relation involving solely the properties of the plasmonic material, and hence of noble metal optical constants [24]. The presence of fundamental limits in optics, however, does not only concern guiding elements: considering intensity modulators, it has been recently highlighted that, when graphene is the active material, the insertion loss of the overall device is substantially governed by the graphene conductivity tensor, according to an inequality proved for planar, multilayered devices embedding conducting sheets [25]. In this article we generalize that result, proving the existence of a lower limit also on the insertion losses introduced by a phase actuator. Moreover, our result applies in general to every two-port device with arbitrary geometry, like realistic structures in integrated optics. Data reported in the literature are critically analyzed in view of the present theory, and the role of resonance in switching devices is highlighted. A material figure of merit, depending solely on the dielectric constant of the switching material,

Dipartimento di Elettronica, Informazione e Bioingegneria, Politecnico di Milano, Piazza Leonardo da Vinci 31, 20133, Milano, Italy
*Corresponding author: e-mail: simone.zanotto@polimi.it

turns out to be the central quantity for both amplitude and phase switches.

## 2. Fundamental limit on the losses of phase actuators

The first problem we address is to determine a fundamental limit on the insertion loss of a phase modulator. A schematic of its simplest implementation is shown in Fig. 1a. It is a two-port linear device that, when passing from state $I$ to state $II$, switches the phase of the output beam by a certain amount. Here we focus on the case of a $\pi$-switch, which is of relevance in most applications. While an ideal phase switch does not act on the amplitude, a real device possibly does that. Such a loss may be due to back-reflection, to scattering into other channels, or to absorption inside the switching region. Following the theory outlined in [25,26], and proved in the Supplementary Material for a device of arbitrary geometry, it turns out that the insertion losses are ultimately determined solely by the complex permittivity of the switching material employed in the device. In formulas:

$$\frac{4\,\min[T_I,\,T_{II}]}{(1-\min[T_I,\,T_{II}])^2} \leq \max_{\mathbf{r}\in V} \frac{|\varepsilon_I(\mathbf{r})-\varepsilon_{II}(\mathbf{r})|^2}{4\,\varepsilon_I''(\mathbf{r})\,\varepsilon_{II}''(\mathbf{r})} \equiv \gamma_{\mathrm{mat}}\,, \tag{1}$$

where $T_I$ and $T_{II}$ are the intensity transmittances of the device in states $I$ and $II$, $\varepsilon_I(\mathbf{r})$ and $\varepsilon_{II}(\mathbf{r})$ are the (complex) permittivities inside the volume $V$ where the switching action takes place, and $\varepsilon''$ denotes the imaginary part of the permittivity. In most of the cases, the difference $\varepsilon_I(\mathbf{r})-\varepsilon_{II}(\mathbf{r})$ is non-zero and constant at the sole spatial locations corresponding to the switching material. Hence, the second term of Eq. (1) only depends on the permittivity, defining a *material figure of merit* independent of the specific device shape. Solving the inequality for $\min[T_I, T_{II}]$, the diagram shown in Fig. 1b is obtained. Here there is a forbidden region which is inaccessible by any device built out of a material which has a given $\gamma_{\mathrm{mat}}$; in other words, it is the switching material that ultimately dictates the minimum amount of losses introduced by the device into the optical path[1]. A material with a small $\gamma_{\mathrm{mat}}$ will necessarily behave as a "bad" actuator, while a material with a large $\gamma_{\mathrm{mat}}$ can potentially be the basis of a well-performing device. A trivial case is that of a transparent material which only changes the real part of the refractive index; in this case, $\gamma_{\mathrm{mat}} \to \infty$, and it is clearly possible to build an ideal phase switch by simply placing the material itself into the optical path. The reverse is more subtle: given a material with $\gamma_{\mathrm{mat}} \to \infty$, a design effort is in general needed to approach the fundamental limit.

To clarify this point, and to check the validity of the general inequality Eq. (1), we analyze the device shown schematically on the right-hand side of Fig. 1b. It simply consists of a waveguide loaded with the switching material; the overlap of the latter with the modal field is $\Gamma$. For a sufficiently weak perturbation[2], the waveguide effective index is modified by $(n+i\kappa)\cdot\Gamma$ in state $I$, and by $(n+\Delta n+i\kappa+i\Delta\kappa)\cdot\Gamma$ in state $II$ [27]. Since the length of the loaded section must be $L_\pi = \lambda_0/2\Gamma\Delta n$, the transmittances in states $I$ and $II$ are given by the formulas shown in Fig. 1b; notice that in these expressions the dependence on $\Gamma$ cancels out. By extracting a random set of $n$, $\Delta n$, $\kappa$, and $\Delta\kappa$, the blue dots in Fig. 1b are obtained. All these points lie in the allowed region of the graph. A detailed observation reveals that there is a narrow area between the forbidden region and the cloud of blue points which is not filled, and two possible causes for this effect have been identified. First, the waveguide perturbation approximation has been assumed here, and this may be weaker in certain areas of the parameter space. Second, the blue dots follow from the analysis of a specific device geometry, i.e. the loaded waveguide; this choice may result in devices which do not reach the optimality boundary in the small $\gamma_{\mathrm{mat}}$ region. Similar behavior is also observed in Section 3 concerning amplitude actuators, and a general solution to that is discussed in detail in Section 4.

Here instead we focus on two cases of special interest, which have been referred to above. One is that of a material which is nearly transparent in both states; its representative point is labeled (i) on the graph in Fig. 1b. Specifically, its parameters are $n=2$, $\Delta n=1$, $\kappa=1.5\times10^{-3}$, $\Delta\kappa=0$. This leads to $\gamma_{\mathrm{mat}}\simeq10^5$ and $T_I=T_{II}=0.99$; that is, a nearly ideal phase delay device with negligible insertion losses. Consider instead a material characterized by $n=2$, $\Delta n=1$, $\kappa=5\times10^{-6}$, $\Delta\kappa=0.5$. Again, the figure of merit is $\gamma_{\mathrm{mat}}\simeq10^5$, but the insertion loss in state $II$ is large: $T_{II}=0.04$ (point (ii)). In essence, when attempting to realize a loaded-waveguide phase actuator device which relies on this material, a very poor performance is obtained. This is because $\Delta\kappa$ is large compared to $\Delta n$, and the loaded-waveguide section mostly works as an amplitude switch.

However, even relying on such a material, it is possible to design a phase switch that approaches the limit given by Eq. (1). Consider for instance the device sketched in Fig. 1c. It consists of a ring resonator filter loaded with the switching material. While the switching material itself essentially acts as an amplitude switch, the global device implements a $\pi$ phase shift actuator. Indeed, in the transparent state, and for resonant wavelengths, the ring behaves as an all-pass filter

[1] It should be highlighted that the limit expressed by Eq. (1) is reached when the main contribution to the total losses is that originating from absorption in the switching material. Hence, the reduction of losses such as reflection and scattering, or dissipation in opaque components other than the switching material, is always beneficial.

[2] The weak perturbation approximation can be safely applied to low-contrast structures; however, finite-element simulations show that it can be applied with good accuracy also to silicon-on-insulator waveguides, provided that the loading material does not introduce a very large perturbation to the cladding index, or that the field overlap with the loading material is small enough.

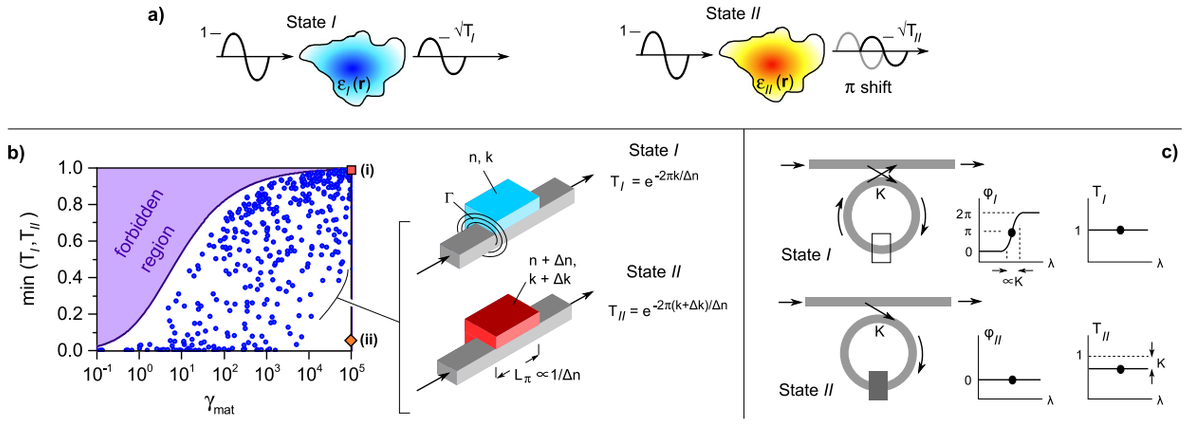


**Figure 1** Fundamental limit for a phase-switching optical element. (a) Schematic of the switching action. (b) Minimum transmission for a $\pi$-switch as a function of the material figure of merit $\gamma_{\rm mat}$. The points describe the action of a simple device consisting of a waveguide loaded with the active material; different points correspond to different parameters $n$, $\Delta n$, $\kappa$, and $\Delta\kappa$. All the devices lie in the allowed region of the chart; however, certain devices are strongly sub-optimal. (c) Possible implementation of an optimized *phase* switch based on a material which has *intensity* switching properties.

which shifts the output phase by $\pi$ (state $I$). In the opaque state, instead, the ring is "broken" and no phase shift appears at the output port (state $II$). This is an example which shows the potentiality of the concept of material figure of merit $\gamma_{\rm mat}$ and of Eq. (1): by an appropriate device design, it is possible to obtain a quasi-ideal phase switch even though at a first glance the material itself is not suited for that purpose. The distance from the zero-insertion-loss condition (IL $\simeq 0 \leftrightarrow T \simeq 1$) is here tuned by a device parameter, the coupling efficiency $K$ (see Fig. 1c): small values of $K$ mean small IL. It should however be noticed that a small $K$, and hence a small IL, is accompanied by a narrow bandwidth, a known tradeoff encountered in optical devices based on resonance.

## 3. Fundamental limit on the losses of amplitude actuators

The second problem we address is that of evaluating the performance of an amplitude switch. Its working principle is shown schematically in Fig. 2a. State $I$ is the "on" of the device, in the sense that light is not blocked; conversely, state $II$ is the "off". An ideal amplitude switch would allow all the radiation pass in state $I$, while completely blocking it in state $II$. Non-idealities are hence described by the IL and by the extinction ratio (ER), usually expressed in dB scale: $\mathrm{IL} = -10\log_{10} T_I$, $\mathrm{ER} = -10\log_{10} T_{II}/T_I$. As for the phase switch, by generalizing the theory reported in Ref. [25], it can be shown that the following inequality holds:

$$\frac{T_I\left(\sqrt{T_I/T_{II}}-1\right)^2}{(1-T_I)(T_I/T_{II}-T_I)} \leq \gamma_{\rm mat}, \qquad (2)$$

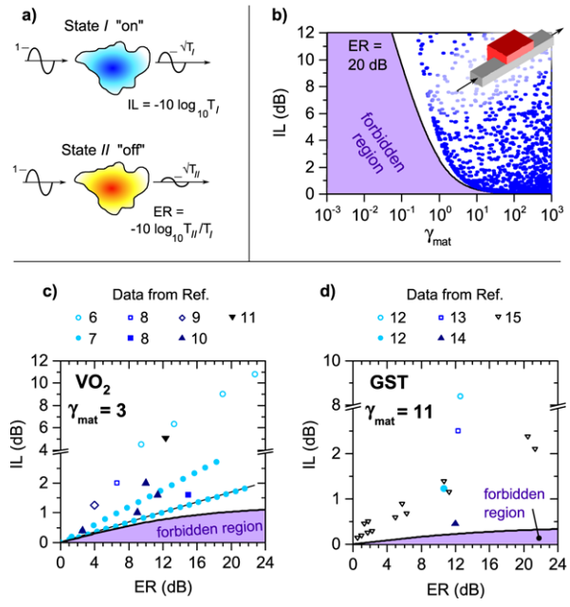


**Figure 2** Fundamental limit for an amplitude-switching optical element. (a) Schematic of the switching action. (b) Minimum insertion loss as a function of the material figure of merit when an extinction ratio of 20 dB is required. The points represent the loss of a loaded-waveguide intensity switching device, where the refractive index and attenuation coefficient of the material in states $I$ and $II$ are randomly chosen. All the points lie in the allowed region. (c) Validation of the theory based on the analysis of literature data for $VO_2$. (d) Same as in (c), but here for GST. In (c) and (d), empty symbols correspond to experimental works, filled symbols to theoretical ones.

where the material figure of merit $\gamma_{\mathrm{mat}}$ only depends on the permittivities of the switching material in states *I* and *II* (see Eq. (1)).

Similarly to the result concerning phase actuators, an intensity actuator relying on a material with small $\gamma_{\mathrm{mat}}$ will have large insertion losses; conversely, if a material with large $\gamma_{\mathrm{mat}}$ is employed, small insertion losses can be obtained. If, for instance, an extinction ratio of 20 dB is required, the limiting curve reported in Fig. 2b applies. Again, the validity of the limit is confirmed by analyzing the performance of the loaded-waveguide device, now designed to act as an intensity switch, in the weak perturbation approximation. Assuming that the complex refractive index of the switching material is $(n + i\kappa)$ in state *I* and $(n + \Delta n + i\kappa + i\,\Delta\kappa)$ in state *II*, under this approximation it is straightforward to show that, to achieve an ER, the insertion loss is $\mathrm{IL} = \mathrm{ER} \cdot \kappa/\Delta\kappa$, independent of the overlap factor $\Gamma$ between the guided mode and the switching material. We extracted a random set of quartets ($n$, $\Delta n$, $\kappa$, $\Delta\kappa$), and represent as a blue dot in Fig. 2b the corresponding pair ($\gamma_{\mathrm{mat}}$, IL). All the dots lie in the allowed region, thus confirming the validity of Eq. (2) over a large span of $\gamma_{\mathrm{mat}}$.

The support for Eq. (2) reported above, however, relies on a quite special device geometry and on the weak perturbation approximation; these are also the reasons why the allowed region is not completely filled by the blue points. How to get closer to the forbidden region is systematically addressed in the next section; here instead we gain further confidence in Eq. (2) by relying on theoretical and experimental results reported in the literature. We have chosen two cases for study: the phase-change materials $VO_2$ and GST. These materials have attracted much attention in recent years, since the huge contrast that characterizes the optical responses of the two states allows the implementation of extremely compact devices, with footprints down to submicrometer size. In addition, devices based on these materials are interesting because of low energy consumption, self-holding operation (in the case of GST), and integrability of the switching material into existing platforms; most markedly, into silicon photonics or in connection with surface plasmons. However, most of these devices suffer from quite large insertion losses, and the question naturally arises as to whether these losses can be eliminated through careful design of the devices and technology improvement, or if they are inherent in employing phase change materials.

In Fig. 2c we plot as dots the insertion losses versus the extinction ratios of several $VO_2$-based devices reported in the literature. Empty symbols correspond to experimental works and filled symbols to theoretical ones. All the representative points lie in the allowed region of the graph. It is worth noticing that the results of theoretical works, and especially that of [7], lie very close to the forbidden region: by relying on $VO_2$, no further improvements are possible. Here we employed the value $\gamma_{\mathrm{mat}} = 3$, which follows from the complex refractive indices reported in [7]; the values reported in the other articles lead to slightly different $\gamma_{\mathrm{mat}}$, but we systematically checked that the corresponding (IL, ER) values lay outside the related forbidden region. Similarly, in Fig. 2d we show a set of IL–ER pairs taken from the literature for GST. Here the forbidden region is narrower, in consequence of the fact that GST has a larger $\gamma_{\mathrm{mat}}$ with respect to $VO_2$. Consistently, there are reports in the literature of device performances close to the fundamental limit [14].

Far from being a complete review of the switching materials employed in integrated optics and nanophotonics, the analyses detailed above show the potentials and limitations of two relevant phase change materials at telecommunications wavelengths, and provide further confirmation of the validity of Eq. (2).

## 4. Resonant versus non-resonant amplitude actuators

It will now be shown that a switching device whose working principle is non-resonant wave propagation through a region loaded by the absorbing material may be quite far from optimality. Consider, for instance, the family of devices whose representative points are highlighted by a straight line in Fig. 2c. These points lie on a straight line since they follow from insertion losses and extinction ratio given per unit length, the device being a plasmonic waveguide loaded with the switching material. Despite the waveguide itself is well optimized (the points are essentially tangent to the curve which delimits the forbidden region), when devices with larger and larger extinction ratio are desired, they turn out to deviate more and more from the fundamental limit. Clearly, this problem is not limited to the $VO_2$-based device of Ref. [7]; rather, it concerns every switching device based on light propagation through the switching region. While this is not an issue as far as single actuators with low extinction ratios are concerned, it may pose a problem in applications where a cascade of actuators or large extinction ratios are needed.

However, following the limit theory, there are no first-principle limitations to realizing a device with insertion losses smaller than those inherent to a component based on wave propagation. Again, as observed above for phase actuators, a key is to base the switch on a resonant element. In Fig. 3 we compare a device based on wave propagation through a simple loaded waveguide with a ring resonator where a section of the loop is replaced by the loaded waveguide. The points describe realistic devices based on a rib silicon waveguide loaded with $VO_2$, whose geometry is taken from [8]. This waveguide is characterized by two complex effective indices, corresponding to the two states of $VO_2$: $n_{\mathrm{eff},I} = 2.92$, $n_{\mathrm{eff},II} = 2.68$, $\kappa_{\mathrm{eff},I} = 0.025$, $\kappa_{\mathrm{eff},II} = 0.112$. For a fixed waveguide geometry, and consequently for a given pair of propagation constants $\beta_{I,II} = 2\pi(n_{\mathrm{eff};I,II} + i\kappa_{\mathrm{eff};I,II})/\lambda_0$, the only relevant device parameter in the propagation configuration is the length. In the resonant configuration, however, there are

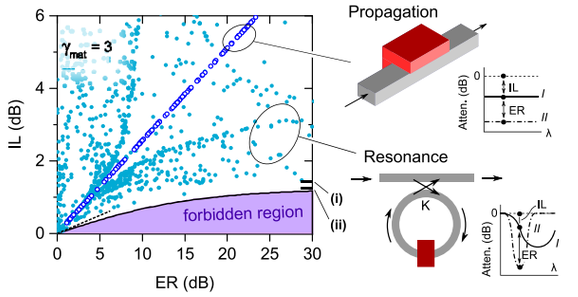


**Figure 3** Performance of propagation-based and resonance-based amplitude actuators in comparison with the fundamental limit. The resonance-based device can perform better than the propagation-based one, especially in the large ER region. Filled and empty dots are obtained by randomly choosing the key parameters for the two geometries (see text). The point marked (i) represents the minimum IL achievable at arbitrarily large ER with the ring-based device. The point marked (ii) represents the minimum IL achievable at arbitrarily large ER for the most general switching device relying on a material with $\gamma_{\mathrm{mat}} = 3$.

two relevant parameters[3]: the loaded section length $L$ and the intensity coupling coefficient $K$. The total ring length is fixed by imposing the resonance condition either in state $I$ or in state $II$. From the point distribution – which follows from a random set of the key parameters $L$ and $K$ – it turns out that, in the large extinction ratio region, the device based on resonance may perform much better than that based on propagation, and that performances very close to the fundamental limit can be obtained. This resonance-mediated approach to the fundamental limit occurs even in the case where the loaded waveguide design by itself is not optimal, which may occur, for instance, due to fabrication constraints. Consider again the data in Fig. 3. Here, the line corresponding to the propagation-based device is not tangent to the forbidden region (the line tangent to the forbidden region, given by $\mathrm{IL} = \mathrm{ER} \cdot (\sqrt{1 + 1/\gamma_{\mathrm{mat}}} - 1)/2$, is highlighted as a dashed line close to the origin of the axes in Fig. 3). Nevertheless, by embedding such a waveguide into a resonant ring, performance much closer to the fundamental limit could be obtained.

Although for illustrative purposes here we analyzed a $VO_2$-based device, the idea that a resonant device is closer to the fundamental limit than a device based on light propagation is demonstrated in a general form in the following. To this end, we notice that, in a resonant device, the large extinction ratio regime is reached under the critical coupling condition. Neglecting the bare waveguide transmission losses, one has $\mathrm{ER} \to \infty$ when the coupling between the bus waveguide and the ring is matched with the transmission loss through the loaded section. Consistent with the notation of Fig. 2, the material state $II$ is chosen as the device "off" state; thus, the critical coupling condition is written $K = 1 - e^{-2\beta''_{II}L}$. Given this constraint, the insertion loss at critical coupling is readily obtained in closed form:

$$\mathrm{IL}_{\mathrm{ring,ER}\to\infty} = -10\log_{10} \times \frac{e^{-2\beta''_I L} + e^{-2\beta''_{II}L} - 2e^{-(\beta''_I+\beta''_{II})L}\cos\left[(\beta'_I - \beta'_{II})L\right]}{1 + e^{-2(\beta''_I+\beta''_{II})L} - 2e^{-(\beta''_I+\beta''_{II})L}\cos\left[(\beta'_I - \beta'_{II})L\right]}. \tag{3}$$

It can be shown (see Supplementary Material) that this expression is minimized when $L \to 0$, i.e. when $K \to 0$, and that the limit value is

$$IL_{\mathrm{ring,ER}\to\infty,\mathrm{min}} = -10\log_{10}\frac{(\beta''_I - \beta''_{II})^2 + (\beta'_I - \beta'_{II})^2}{(\beta''_I + \beta''_{II})^2 + (\beta'_I - \beta'_{II})^2}. \tag{4}$$

The existence of this limit, and the fact that it is finite, is a proof that a critically coupled ring resonator device always outperforms a propagating-wave device, as long as large extinction ratios are considered. The proof given in the Supplementary Material also supports that this conclusion is independent of the specific material under consideration. For the specific case of the $VO_2$-based device analyzed above, this limit is shown as the point marked (i) in Fig. 3. Consistently, this limit lies below all the points representing the resonant devices at large extinction ratios, while it is above the fundamental limit

$$\mathrm{IL}_{\mathrm{fund,ER}\to\infty} = -10\log_{10}\frac{\gamma_{\mathrm{mat}}}{1+\gamma_{\mathrm{mat}}} \tag{5}$$

obtained from Eq. (2) and labeled (ii) in Fig. 3.

It should be noticed that the limit in Eq. (5) involves the bulk material permittivity (in the case of Fig. 3, $VO_2$), while that in Eq. (4) involves the propagation constant of the considered waveguide design (in the case of Fig. 3, that of Ref. [8]). However, it is proved in the Supplementary Material that the limit in Eq. (4) is always larger than that in Eq. (5), independent of the specific choice of the switching material and of the waveguide geometry. As already noted in Section 2 for phase actuators, the use of resonant components has the drawback that the bandwidth is in general reduced with respect to the case of propagation-based devices. Anyway, as far as the optimality with respect to insertion losses are concerned, the results given above together with those given in Section 2 support the conclusion that the concept of resonance may play a crucial role in the optimization of optical actuators. Although the discussion in the present article deals with integrated optical waveguides and ring resonators, the generality of the resonance and critical coupling concepts allows extrapolation of the

[3] A more refined model would include, for instance, reflection and scattering at the unloaded/loaded waveguide interface, and distributed backscattering. However, since these loss mechanisms can be reduced by appropriate engineering, and since the aim is here to analyze the *intrinsic* limits of actuators, these losses are not included in the model.

present results also to other photonic platforms such as photonic crystals and metamaterials [28, 29].

We conclude this section by noticing that the above analysis does not depend on the choice of the material "transparent" state as state *I* and "opaque" state as state *II*, or vice versa. In the deduction of Eq. (2), indeed, this assumption has not been made, and the designer is free to choose the switching material "opaque" state for the device "on" state (i.e. the device state which does not block light flow), or the opposite. This fact may be exploited in view of energy saving. Suppose that the need is to design a device intended for normally-on operation, and that the switching material has one of the two states which is power-hungry. The device can be engineered to use the power-hungry material state for the device "off" state, hence reducing the overall energy consumption. While this conclusion is general and holds for arbitrary device geometry, it can be read out directly in the framework of a critically coupled ring resonator by noticing that Eqs. (3) and (4) are invariant for the exchange $I \leftrightarrow II$.

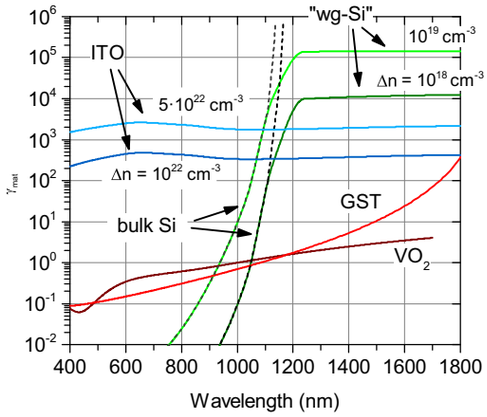


**Figure 4** Spectral dependence of the figure of merit $\gamma_{mat}$ for four materials employed in nanophotonics, whose working principles are different. Dielectric modulation in $VO_2$ and GST is due to a phase transition, while in ITO and silicon the plasma effect due to free carriers is considered. In silicon, for wavelengths longer than the bandgap, extrinsic losses due to waveguide scattering are included.

## 5. Comparison of various materials employed in actuators

The power of the limits expressed by the inequalities given in Eqs. (1) and (2) is that it is sufficient to know the figure of merit $\gamma_{mat}$ of the (bulk) switching material to have significant insights into the potentiality of a new material, prior to directly designing specific devices. Furthermore, the limits may be of help as far as an optimization is concerned, when the decision whether to proceed with further optimization steps has to be taken. It is clear that the inequalities given above and the material figure of merit only provide information on a single metric of the device performance, while other issues like bandwidth, footprint, switching energy, state retention, switching time, etc., are not encompassed by $\gamma_{mat}$. Nevertheless, knowledge of $\gamma_{mat}$ could be of help, for instance, in choosing the material that is best suited for operation in a certain wavelength range. Indeed, $\gamma_{mat}$ only depends on the permittivities, which are often known from optical reflectometry or ellipsometry, from first-principles structural calculations, or from other models.

In Fig. 4 we propose a spectral comparison, regarding two phase change materials (GST and $VO_2$), a transparent conductive oxide (ITO), and a semiconductor (silicon). In the phase change materials, the permittivity change is induced by a structural transition – amorphous to crystalline in the case of GST and from a monoclinic to a rutile structure in the case of $VO_2$. The dielectric functions are retrieved from [30, 31]. In the case of ITO, the plasma dispersion effect modeled by a Drude contribution to the permittivity is responsible for the modulation effect. Here, typical parameters for the dielectric response are taken from [18,19,32–34] and correspond to a mobility of 15 cm$^2$/(V s). In contrast to the phase change materials, whose response is intrinsic to their structure (a change in certain optical matrix elements for GST [35] and a semiconductor–insulator Mott transition for $VO_2$ [36]), the plasma effect in ITO can be tuned through the electron population injected or accumulated in the active region. It turns out that the material figure of merit $\gamma_{mat}$ significantly depends on that parameter, gaining more than one order of magnitude over a wide spectral range for an order-of-magnitude change in the electron density.

The plasma dispersion effect is also at the origin of the response of silicon [37], and is here quantified assuming a mobility of 1500 cm$^2$/(V s), and an injected electron density of $10^{18}$ or $10^{19}$ cm$^{-3}$. By introducing also the effect of holes the figure of merit is increased by a factor $\sim 2$. As opposed to the other materials, which have a flat response in a wide spectral range, silicon strongly feels the effect of a bandgap. If the bulk silicon permittivity is employed, in the "undoped" state the material is well transparent, implying values of $\gamma_{mat}$ larger than $10^6$ above a wavelength of 1.2 $\mu$m. However, when silicon is employed for optical waveguides, extrinsic losses due to roughness scattering and surface state absorption always occur. These losses, despite being extrinsic to the bulk material, and rather connected to the device itself, can however be accounted for in the material figure of merit, defining a $\gamma_{mat}$ for an effective "waveguide silicon" material. Assuming a loss of 1 dB/cm [38], values of $\gamma_{mat} = 10^4$–$10^5$, flat in the whole near-infrared spectral range, are obtained. If instead a low-loss 0.1 dB/cm silicon waveguide is considered [39], the material figure of merit increases by an order of magnitude. As for ITO, also for silicon the figure of merit depends significantly on the injected charge density. Hence, provided that the mobility is not reduced when a large charge density is involved, it is convenient to work in this regime. This is a consequence of the balance between the real and imaginary part of the permittivity given by the Drude model, and applies to every material whose switching action relies on this mechanism.

## 6. Conclusions and perspectives

In conclusion, we derived fundamental limits on the losses of arbitrarily shaped two-port amplitude and phase optical actuators. Finding their roots in a simple manipulation of Maxwell's equations for linear and reciprocal dielectrics, the validity of these limits extends to a wealth of linear switching devices, and in particular to integrated optics devices regardless of the specific geometric configuration. The key role is played by the switching material, whose effectiveness is quantified by a material figure of merit simply defined in terms of the permittivities. While the introduced figure of merit does not give insights into certain metrics like switching time, footprint, state retention, switching energy, etc., it sets clear limits on the optical performances of any device which relies on a given material. Further, we observed a peculiar connection between the ability to reach the fundamental limit and the presence of resonance and of critical coupling in the operation principle of a device. We believe that the present theory provides an important metric tool which will direct researchers towards high-performance optical devices and materials.

## Supporting Information

Additional supporting information may be found in the online version of this article at the publisher's website.

**Acknowledgement.** The research leading to these results received funding from the EU Seventh Framework Programme (FP7/2007-2013) under grant agreement no. 323734 "Breaking the Barrier on Optical Integration" (BBOI). Fruitful discussions with Daniele Melati and Marco Morandotti are also gratefully acknowledged.

**Received:** 20 April 2015, **Revised:** 10 July 2015,
**Accepted:** 5 August 2015

**Published online:** 23 September 2015

## References

[1] W. Shockley and H. J. Queisser, J. Appl. Phys. **32**, 510–519 (1961).
[2] E. Yablonovitch, J. Opt. Soc. Am. **72**, 899–907 (1982).
[3] Z. Yu, A. Raman, and S. Fan, Phys. Rev. Lett. **109**, 173901 (2012).
[4] D. A. Miller, Photon. Res. **1**, 1–15 (2013).
[5] A. Peruzzo, J. McClean, P. Shadbolt, M. H. Yung, X. Q. Zhou, P. J. Love, A. Aspuru-Guzik, and J. L. O'Brien, Nature Commun. **5**, 4213 (2014).
[6] A. Joushaghani, B. A. Kruger, S. Paradis, D. Alain, J. Stewart Aitchison, and J. K. S. Poon, Appl. Phys. Lett. **102**, 061101 (2013).
[7] B. A. Kruger, A. Joushaghani, and J. K. S. Poon, Opt. Express **20**, 23598–23609 (2012).
[8] R. M. Briggs, I. M. Pryce, and H. A. Atwater, Opt. Express **18**, 11192–11201 (2010).
[9] J. D. Ryckman, V. Diez-Blanco, J. Nag, R. E. Marvel, B. K. Choi, R. F. Haglund, and S. M. Weiss, Opt. Express **20**, 13215–13225 (2012).
[10] K. J. Ooi, P. Bai, H. S. Chu, and L. K. Ang, Nanophotonics **2**, 13–19 (2013).
[11] A. Joushaghani, J. Jeong, S. Paradis, D. Alain, J. S. Aitchison, and J. K. S. Poon, Opt. Express **23**, 3657–3668 (2015).
[12] D. Tanaka, Y. Shoji, M. Kuwahara, X. Wang, K. Kintaka, H. Kawashima, T. Toyosaki, Y. Ikuma, and H. Tsuda, Opt. Express **20**, 10283–10294 (2012).
[13] M. Rudé, J. Pello, R. E. Simpson, J. Osmond, G. Roelkens, J. J. van der Tol, and V. Pruneri, Appl. Phys. Lett. **103**, 141119 (2013).
[14] W. H. P. Pernice and H. Bhaskaran, Appl. Phys. Lett. **101**, 171101 (2012).
[15] C. Rios, P. Hosseini, C. D. Wright, H. Bhaskaran, and W. H. P. Pernice, Adv. Mater. **26**, 1372–1377 (2014).
[16] M. Rudé, R. E. Simpson, R. Quidant, V. Pruneri, and J. Renger, ACS Photon. **2**, 669–674 (2015).
[17] A. K. U. Michel, D. N. Chigrin, T. W. W. Maß, K. Schönauer, M. Salinga, M. Wuttig, and T. Taubner, Nano Lett. **13**, 3470–3475 (2013).
[18] C. Huang, R. J. Lamond, S. K. Pickus, Z. R. Li, and V. J. Sorger, IEEE Photon. J. **5**, 2202411 (2013).
[19] E. Feigenbaum, K. Diest, and H. A. Atwater, Nano Lett. **10**, 2111–2116 (2010), PMID: 20481480.
[20] A. Melikyan, L. Alloatti, A. Muslija, D. Hillerkuss, P. Schindler, J. Li, R. Palmer, D. Korn, S. Muehlbrandt, D. Van Thourhout, B. Chen, R. Dinu, M. Sommer, C. Koos, M. Kohl, W. Freude, and J. Leuthold, Nature Photon. **8**, 229–233 (2014).
[21] C. Hoessbacher, Y. Fedoryshyn, A. Emboras, A. Melikyan, M. Kohl, D. Hillerkuss, C. Hafner, and J. Leuthold, Optica **1**, 198–202 (2014).
[22] K. Liu, C. R. Ye, S. Khan, and V. J. Sorger, Laser Photon. Rev. **9**, 172–194 (2015).
[23] N. Kinsey, M. Ferrera, V. M. Shalaev, and A. Boltasseva, J. Opt. Soc. Am. B **32**, 121–142 (2015).
[24] A. Arbabi, E. Arbabi, and S. Safavi-Naeini, arXiv preprint arXiv:1411.4402 (2014).
[25] M. Tamagnone, A. Fallahi, J. R. Mosig, and J. Perruisseau-Carrier, Nature Photon. **8**, 556–563 (2014).
[26] T. Schaug-Pettersen and A. Tonning, IRE Trans. Circuit Theory **6**, 150–158 (1959).
[27] A. W. Snyder and J. Love, Optical Waveguide Theory (Springer Science & Business Media, 1983).
[28] F. Du, Y. Q. Lu, and S. T. Wu, Appl. Phys. Lett. **85**, 2181–2183 (2004).
[29] A. Boardman, V. Grimalsky, Y. Kivshar, S. Koshevaya, M. Lapine, N. Litchinitser, V. Malnev, M. Noginov, Y. Rapoport, and V. Shalaev, Laser Photon. Rev. **5**, 287–307 (2011).
[30] H. Kakiuchida, P. Jin, S. Nakao, and M. Tazawa, Japn. J. Appl. Phys. **46**, L113 (2007).
[31] J. Orava, T. Wágner, J. Šik, J. Přikryl, M. Frumar, and L. Beneš, J. Appl. Phys. **104**, 043523 (2008).

[32] J. A. Dobrowolski, F. C. Ho, and A. Waldorf, Appl. Opt. **22**, 3191–3200 (1983).
[33] F. Michelotti, L. Dominici, E. Descrovi, N. Danz, and F. Menchini, Opt. Lett. **34**, 839–841 (2009).
[34] Y. S. Jung, Thin Solid Films **467**, 36–42 (2004).
[35] S. Caravati, M. Bernasconi, and M. Parrinello, J. Phys.: Condens. Matter **22**, 315801 (2010).
[36] M. M. Qazilbash, M. Brehm, B. G. Chae, P. C. Ho, G. O. Andreev, B. J. Kim, S. J. Yun, A. Balatsky, M. Maple, F. Keilmann, H. T. Kim, and D. Basov, Science **318**, 1750–1753 (2007).
[37] R. A. Soref and B. R. Bennett, IEEE J. Quantum Electron. **23**, 123–129 (1987).
[38] F. Morichetti, A. Canciamilla, C. Ferrari, M. Torregiani, A. Melloni, and M. Martinelli, Phys. Rev. Lett. **104**, 033902 (2010).
[39] A. Biberman, M. J. Shaw, E. Timurdogan, J. B. Wright, and M. R. Watts, Opt. Lett. **37**, 4236–4238 (2012).